INFECTION AND IMMUNITY, Apr. 2008, p. 1379–1389 Vol. 76, No. 4
0019-9567/08/$08.00+0 doi:10.1128/IAI.00745-07

NK Cells and Gamma Interferon Coordinate the Formation and Function of Hepatic Granulomas in Mice Infected with the *Francisella tularensis* Live Vaccine Strain▽

Sirosh M. Bokhari,[1] Kee-Jun Kim,[1] David M. Pinson,[2] Joyce Slusser,[1] Hung-Wen Yeh,[3] and Michael J. Parmely[1]*

Department of Microbiology, Molecular Genetics and Immunology,[1] Department of Pathology and Laboratory Medicine,[2] and Department of Biostatistics,[3] University of Kansas Medical Center, Kansas City, Kansas 66160

Received 1 June 2007/Returned for modification 30 July 2007/Accepted 11 January 2008

Host innate immune responses to many intracellular pathogens include the formation of inflammatory granulomas that are thought to provide a physical barrier between the microbe and host. Because two common features of infections with the live vaccine strain (LVS) of *Francisella tularensis* within the mouse liver are the formation of granulomas and the production of gamma interferon (IFN-γ), we have asked what role IFN-γ plays in hepatic granuloma formation and function. *Francisella* antigens were predominantly localized within granulomas of the livers of mice infected with *F. tularensis* LVS 4 days postinfection. Hepatic granulomas also contained large numbers of dying cells, some of which coexpressed the F4/80 macrophage antigen and activated caspase-3. IFN-γ-deficient mice did not form normal numbers of hepatic granulomas and showed widely disseminated *Francisella* antigens within the liver. The incidence of cell death within hepatic granulomas also decreased significantly in the absence of IFN-γ. Inducible NO synthase (iNOS) expression was restricted to the granulomas of wild-type mice but was not seen for IFN-γ-deficient mice. Cell death within granulomas was also significantly decreased for iNOS-deficient mice. The predominant IFN-γ-expressing cells in the liver were NK cells. Depleting NK cells resulted in the expression of bacterial antigens and iNOS outside the granulomas and the appearance of extensive hepatic focal necrosis. These findings indicate that IFN-γ and hepatic NK cells that are activated during *F. tularensis* LVS infections regulate hepatic granuloma formation, the spatial containment of infection, the expression of iNOS, and the induction of cell death within the liver.

Tularemia is a zoonotic infectious disease caused by the facultative intracellular bacterium *Francisella tularensis*. The initial clinical presentation and dominant features of this condition reflect the mode of transmission and the route of infection. The ulceroglandular form, most frequently acquired from bites of arthropods, is characterized by an initial papular skin lesion that can progress to an eschar or ulcer with regional lymphadenopathy. Inhalation of aerosolized bacteria or secondary hematogenous dissemination of infection to the lungs results in pneumonic tularemia characterized by fever, a broad range in the severity of respiratory symptoms, and a high mortality rate. In the so-called "typhoidal" form of tularemia, patients present with similar systemic symptoms without a clear focus of primary infection. They may show sepsis and rhabdomyolysis with multiorgan system failure, including renal impairment. Following pulmonary and gastrointestinal infection, systemic dissemination of the pathogen leads to the colonization of the liver, where organisms infect both macrophages and hepatocytes (4, 6). At autopsy, the livers of infected human beings often show areas of focal coagulation necrosis throughout the parenchyma of the organ (18).

The infection of mice with the live vaccine strain (LVS) of *F. tularensis* subsp. *holarctica* is a commonly used animal model and is associated with the formation of multifocal hepatic microgranluomas containing $CD11b^+$ macrophages and $Gr\text{-}1^+$ $CD11b^+$ immature myeloid cells followed in time by the appearance of hepatic focal necrosis (25). Neither the process of granuloma formation nor the function of these structures has been systematically studied, and we know little about the determinants of the pathogen or the host that promote their formation or regulate their functions. The induction of granulomas in infected tissues is a property shared by several intracellular microbial pathogens, including *Mycobacterium tuberculosis*, *Listeria monocytogenes*, *Schistosoma mansoni*, *Leishmania donovani*, and *Histoplasma capsulatum* (11, 13–16, 26, 27, 30). In general, the tissue remodeling that facilitates the formation of a granuloma has been seen as an attempt by the host to separate itself from the pathogen, physically isolating the microbe with a layer of inflammatory cells and preventing microbial dissemination. Granulomas also serve as foci for recruiting and concentrating antimicrobial defenses while spatially limiting inflammatory or microbial host tissue damage (22).

Chen et al. (2) first reported that gamma interferon (IFN-γ)-deficient mice show decreased hepatic granuloma formation in response to challenge with virulent type B *F. tularensis* organisms. Thus, the IFN-γ-deficient mouse provides an experimental model with which two important issues can be addressed. The first is the role of IFN-γ in controlling the spatial distribution of the pathogen within the liver. Second, by characterizing the distribution of hepatic cell death in this mutant mouse, one can infer the likely role of granulomas in restricting tissue damage during *F. tularensis* infection.

* Corresponding author. Mailing address: Department of Microbiology, Molecular Genetics and Immunology, University of Kansas Medical Center, 3901 Rainbow Blvd., Kansas City, KS 66160. Phone: (913) 588-7053. Fax: (913) 588-7295. E-mail: mparmely@kumc.edu.

▽ Published ahead of print on 28 January 2008.

Accordingly, the current study was designed to determine which, if any, of the functions typically associated with infectious granulomas are provided by these structures in the livers of *F. tularensis* LVS-infected mice. When lethal doses of the pathogen are given by the intranasal (i.n.) route, the liver is consistently colonized, presumably by the hematogenous spread of infection from the lungs. Using this model, we have asked four important questions about the hepatic granulomas that are seen for *F. tularensis* LVS-infected mice. (i) Are granulomas essential for mounting an effective antimicrobial response against the pathogen in the liver? (ii) Do hepatic granulomas spatially limit the infection within the liver? (iii) Do granulomas spatially limit host cell death and hepatic tissue damage? (iv) Does inducible nitric oxide synthase (iNOS) mediate any of the functions of developing hepatic granulomas in *F. tularensis* LVS-infected mice? The impaired ability of infected IFN-γ-deficient mice to form hepatic granulomas has provided an experimental model with which we have addressed each of these questions.

MATERIALS AND METHODS

Reagents. The following fluorochrome-labeled antibodies were obtained from BD Biosciences (San Jose, CA) and used in flow cytometry: allophycocyanin-conjugated mouse anti-mouse NK1.1, R-phycoerythrin-Cy7-conjugated hamster anti-mouse CD3ε, and phycoerythrin-conjugated rat anti-mouse IFN-γ. Unconjugated anti-CD16/CD32 was used for blocking Fc receptors. GolgiPlug containing brefeldin A for blocking protein transport, CytoFix/CytoPerm, and Perm/Wash buffer were purchased from BD Biosciences. Ethidium monoazide bromide (EMA) (Invitrogen, Carlsbad, CA) was used to stain dead cells prior to flow cytometry.

Rabbit anti-mouse asialo-GM1 was obtained from Wako Chemicals USA, Inc. (Richmond, VA). The following antibodies were used for immunoperoxidase staining of tissue sections: rabbit anti-*F. tularensis* LVS, which was produced against an inactivated whole-cell preparation (BD Diagnostic Systems, Sparks, MD); goat anti-mouse CD3ε (Santa Cruz Biotechnology, Santa Cruz, CA); rabbit anti-mouse iNOS (Santa Cruz); and biotinylated donkey anti-goat immunoglobulin G (IgG) (Invitrogen, Carlsbad, CA). A rabbit Histostain-SP kit (Zymed Laboratories Invitrogen, Carlsbad, CA) was used for immunoperoxidase staining. For immunofluorescence studies, rat anti-F4/80 was obtained from eBioscience (San Diego, CA), rabbit anti-activated mouse caspase-3 was purchased from Cell Signaling Technologies (Danvers, MA), and Alexa Fluor 488-conjugated and Alexa Fluor 568-conjugated secondary antibodies were obtained from Molecular Probes-Invitrogen (Carlsbad, CA). The TACS terminal deoxynucleotidyltransferase (TdT) kit (R&D Systems, Minneapolis, MN) was used for the detection of dying cells in tissue sections.

Percoll (GE Healthcare, Piscataway, NJ), ACK lysis buffer (Cambrex, Walkersville, MD), DNase, and Liberase (Roche, Indianapolis, IN) were used in preparing mononuclear cells from mouse livers and lungs. Tissue freezing medium (TFM) was from Electron Microscopy Sciences (Hatfield, PA), Vectashield mounting medium was purchased from Vector Laboratories (Burlingame, CA), and 4′,6′-diamidino-2-phenylindole (DAPI) was obtained from Molecular Probes-Invitrogen.

Mice. Six-week-old mice of the following strains were purchased from Jackson Laboratories (Bar Harbor, ME) and used when they were from 7 to 12 weeks of age: C57BL/6J, IFN-γ deficient C57BL/6J.129S7-*Ifng*^{tm1Ts}/J, T-cell-receptor (TCR)-deficient C57BL/6J.129P2-*tcrb*^{tm1Mom}*tcrd*^{tm1Mom}/J, iNOS-deficient C57BL/6J.129P2-*Nos2*^{tm1Lau}/J, and perforin-deficient C57BL/6J-*Prf1*^{tm1Sdz}/J. Mice were housed in autoclaved cages on a 12-h-light/12-h-dark cycle with sterile food and water provided ad libitum. All protocols were approved by the University of Kansas Medical Center Animal Care and Use Committee.

Bacteria. *F. tularensis* LVS was obtained from Jeannine Petersen (Centers for Disease Control and Prevention, Fort Collins, CO). Growth of the organism has been described in detail previously (31). Aliquots of *F. tularensis* LVS were stored frozen without glycerol at −70°C for up to 3 months. Samples were thawed rapidly at 37°C, washed once with Dulbecco's phosphate-buffered saline (DPBS), and resuspended in DPBS for injection. The actual numbers of bacteria injected were determined by dilution plating on chocolate agar.

Mouse infection models. Mice were challenged with *F. tularensis* LVS by either the i.n. or the intraperitoneal route. For i.n. injections, mice were anesthetized with a mixture of ketamine-HCl and xylazine (Phoenix Scientific, Inc., St. Joseph, MO) administered by the intramuscular route. Then, 10 μl of bacterial suspension was inoculated into one nostril followed by an equal volume of DPBS. For tissue collection, mice were again anesthetized, and blood was collected aseptically by cardiac puncture. Total body and organ weights were determined to permit calculation of bacterial burden in each organ. In calculating total blood volume, it was assumed that the blood volume constituted 6% of the body weight.

Rabbit anti-asialo-GM1 was used to deplete NK cells and NKT cells. Mice were injected intraperitoneally with 1.6 mg of anti-asialo-GM1 1 day after infection and with 800 μg of the same antibody on days 2 and 3 postinfection. Tissues were collected on day 4.

Preparation of hepatic, pulmonary, and splenic mononuclear cells. Isolated livers and lungs were washed once in Hanks' balanced salt solution (HBSS) containing 10 mM HEPES and transferred to 5 ml of a digestion buffer (HBSS, 10 mM HEPES, 80 μg/ml of DNase, 50 mg/ml of Liberase). They were then minced finely with scissors. The minced tissues were incubated at 37°C for 15 min and homogenized in an aerosol-free tissue homogenizer (Stomacher 80 Biomaster; Seward, West Sussex, United Kingdom). The enzymes in the mixture were then inhibited by the addition of an equal volume of HBSS containing 10 mM HEPES and 10% fetal bovine serum. Mononuclear cells were isolated by centrifugation over 28% Percoll as previously described (31). After centrifugation, the pellet was resuspended in prewarmed ACK lysis buffer and incubated at 37°C for 3 min to lyse red blood cells. Spleen mononuclear cells were isolated by gentle teasing of the organ with a scalpel blade in HBSS containing 10 mM HEPES, and the erythrocytes were removed by treatment with ACK lysis buffer.

Flow cytometry. Cells were stained for flow cytometry according to the method of Wickstrum et al. (31) with the following modifications. GolgiPlug was included in all buffers (e.g., digestion buffer, Percoll, and ACK lysis buffer) at a concentration of 0.2 μl per ml. Following erythrocyte lysis, the isolated mononuclear cells were resuspended in RPMI 1640 containing 10% fetal bovine serum, penicillin (100 units per ml), streptomycin (100 μg per ml), and GolgiPlug (1 μl per ml) and incubated for 3 h at 37°C in an atmosphere of 5% CO_2. Cells were washed once and resuspended in 1 ml of staining buffer (DPBS with 2% fetal bovine serum). After being counted, the cells were incubated with anti-CD16/CD32 (1 μg/10^6 cells) to block FcγII/III receptors. Fluorochrome-labeled antibodies to NK1.1 and CD3ε were added to cells along with 0.5 μg/ml of EMA, and the mixtures were incubated for 10 min on ice in the dark. The cell suspensions were then exposed to direct fluorescent light for 15 min at room temperature (7, 23). Following two washes with staining buffer, cells were fixed and permeabilized with CytoFix/CytoPerm, washed, and stained with anti-IFN-γ to detect intracellular cytokine. The cells were analyzed on an LSR II flow cytometer (BD Biosciences) using FACSDiva software after gating to exclude EMA-positive cells.

Immunohistology and TdT-mediated dUTP-biotin nick end labeling (TUNEL) staining. Five-micrometer sections were prepared from paraformaldehyde-fixed, paraffin-embedded liver tissues as previously described (29). Sections were stained with antibodies specific for *F. tularensis* LVS, CD3ε, and iNOS by use of a rabbit Histostain-SP kit according to the manufacturer's instructions. For detection of CD3ε, the deparaffinized sections were first boiled in 10 mM citrate buffer, pH 6, for 20 min. Endogenous tissue peroxidase activity was quenched by treatment with 3% hydrogen peroxide in methanol for 10 min. Sections were then blocked with kit blocking buffer (for *F. tularensis* LVS and iNOS) or normal donkey serum (for CD3ε) followed by incubation in primary antibody for 2 h. After being washed in PBS, sections were incubated in biotinylated secondary antibody (for *F. tularensis* LVS and iNOS) or donkey anti-goat IgG (for CD3ε) for 1 h. Bound secondary antibodies were detected using horseradish peroxidase-conjugated streptavidin, and reactions were visualized with aminoethyl carbazole as the substrate. Sections were counterstained with hematoxylin and mounted with GVA mount (Zymed Laboratories Invitrogen, Carlsbad, CA).

Apoptotic cells were detected in tissue sections by TUNEL of cleaved double-strand DNA by use of a TACS TdT kit according to the manufacturer's instructions. Deparaffinized and rehydrated liver sections were first treated with 3% hydrogen peroxide and then permeabilized with proteinase K. Sections were then sequentially treated with TdT, biotinylated nucleotides, and horseradish peroxidase-conjugated streptavidin and developed in diaminobenzidine solution. Sections were counterstained with methyl green. The numbers of TUNEL$^+$ cells were determined by microscopic examination of at least 25 high-power fields (magnification of ×400; area, 0.125 mm^2).

For immunofluorescence colocalization of F4/80 and activated caspase-3, liver tissues were first fixed with 3% paraformaldehyde for 1.5 h. Tissues were then sequentially overlaid at room temperature for 1 h each on sucrose at 5%, 10%, and 15% concentrations. The tissues were transferred to a 1:1 mixture of 15%

sucrose and TFM and embedded in TFM on dry ice. Cryostat sections were treated with ice-cold acetone for 10 min, air dried, and rehydrated in PBS. Following blocking with goat serum, the sections were stained with primary antibodies for 6 h followed by incubation in secondary Alexa Fluor 568-conjugated anti-rat IgG and Alexa Fluor 488-conjugated anti-rabbit IgG for 1 h. The sections were mounted with Vectashield mounting solution containing DAPI and examined with a fluorescence microscope (Nikon Instruments Inc., Melville, NY) equipped with a charge-coupled-device camera. Captured images were processed using Metamorph software, version 7 (Molecular Devices Corporation, Sunnyvale, CA).

Serum IFN-γ levels. Concentrations of IFN-γ in serum were determined by enzyme-linked immunosorbent assay (OptEIA mouse IFN-γ microtiter enzyme-linked immunosorbent assay; BD Biosciences, San Jose, CA) according to the manufacturer's protocol. Microtiter plates were read using a Biotek EL340 reader, and the results are reported as means and standard deviations as determined by DeltaSOFT II software.

Statistics. All experiments were performed at least twice, and the most representative data are shown. Values shown are means and standard deviations. Two-sample *t* tests were applied (see Fig. 3B, 4B, and 6C below) to examine differences in bacterial burdens (log-transformed CFU), frequencies of granulomas, and numbers of TUNEL$^+$ cells inside and outside the granulomas and in both combined. One-way analysis of variance was used to examine differences among the three groups as shown below (see Fig. 6C). The repeated-measurements model was applied (see Fig. 6C) to compare serum IFN-γ levels.

RESULTS

Hepatic infection and granuloma formation follow i.n. challenge of mice with *F. tularensis* LVS. To characterize the inflammatory response in the liver to infection with *F. tularensis* LVS, we first challenged mice with various numbers of the pathogen by the i.n. route and recorded deaths. The 50% lethal dose (LD_{50}) was approximately 500 CFU, and the mean time of death was 8.9 days for mice challenged with 10^3 CFU (Fig. 1A). As observed by others (5, 12), the greatest bacterial burdens during the first week of infection were found in the lungs, but the liver and spleen were important secondary sites of infection, presumably acquired by the hematogenous spread of the organism (Fig. 1B).

Significant colonization of the liver with *F. tularensis* LVS occurred by the third day postinfection and resulted in the formation of multifocal microgranulomas (Fig. 2A). Rasmussen et al. (25) have shown that these inflammatory foci contain cells that express surface markers characteristic of macrophages and immature myeloid precursors. The granulomas increased in frequency and size during the first week postinfection (Fig. 2A and C) and began to merge with one another by the end of the first week. By day 4, cells with a homogeneous eosinophilic cytoplasm showing pyknosis and karyolysis appeared near the outer margins of the granulomas (Fig. 2A, inset). Immunofluorescence colocalization studies (Fig. 2B) indicated that activated caspase-3, an early marker of apoptosis, was expressed by numerous cells within the granulomas as early as day 2 postinfection, and a significant proportion of these cells also expressed the macrophage marker F4/80. By day 4, F4/80$^+$ cells were more difficult to detect, although the frequency of cells expressing activated caspase-3 remained high.

Infection and cell death in the liver are spatially restricted to the microgranulomas. *Francisella* antigens, detected by immunoperoxidase staining, were primarily localized within the granulomas, although occasional hepatocytes outside the granulomas also showed positive staining (Fig. 2A). Cells showing TUNEL staining, indicative of double-strand DNA breaks, were frequently seen near the margins of the granulomas by day 3 and reached their highest densities on day 6 (Fig. 2C). By day 4, approximately 75% of the TUNEL$^+$ cells were found within the granulomas, with the remainder being dispersed throughout the parenchyma of the liver. These findings indicate that bacterial antigens and cell death were found predominantly within granulomas and encouraged us to determine whether IFN-γ, which is known to regulate granuloma formation in *F. tularensis* LVS-infected mice, determined the spatial distribution of bacteria or dying cells.

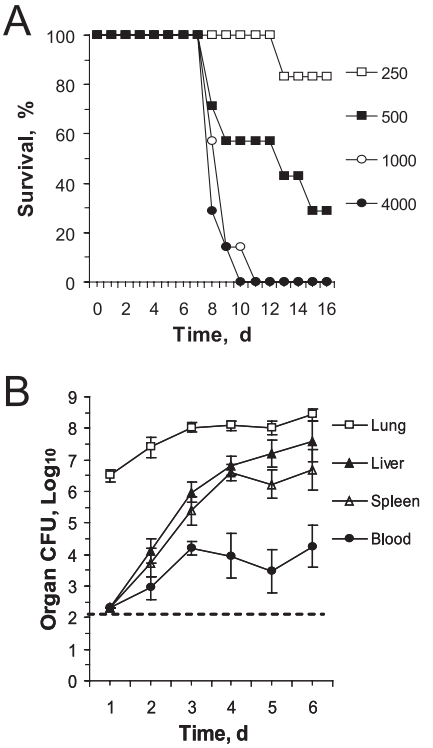

FIG. 1. i.n. infection model. (A) To determine the LD_{50} for mice infected by the i.n. route, C57BL/6J mice (six or seven per group) were challenged with the indicated numbers of viable *F. tularensis* LVS bacteria. (B) Five mice per group were challenged i.n. with 3.6×10^3 CFU *F. tularensis* LVS bacteria, the indicated tissues were collected daily, and total bacterial counts were determined. The horizontal dashed line represents the limit of detection of the assay. d, day.

Production of IFN-γ is essential for granuloma formation, the spatial restriction of infection, and the distribution of cell death within the liver. Wild-type and IFN-γ-deficient mice were challenged with *F. tularensis* LVS and their livers were recovered 4 days postinfection. As reported previously by Chen et al. (2), IFN-γ-deficient mice showed a marked decrease in the numbers of hepatic granulomas, and the granulomas seen for these mutant mice were much smaller than those of infected wild-type animals (Fig. 3A). The numbers of bacteria in the livers and blood of IFN-γ-deficient mice 4 days postinfection were 100 to 1,000 times higher than the levels seen for wild-type mice (Fig. 3B). More importantly, *Francisella* antigens were widely distributed throughout the livers of the IFN-γ-deficient mice rather than being contained primarily within hepatic granulomas (Fig. 3A). The microbial antigens of *F. tularensis* LVS were evident within hepatic sinusoids, numerous hepatocytes (Fig. 3A, inset), and Kupffer cells of the mu-

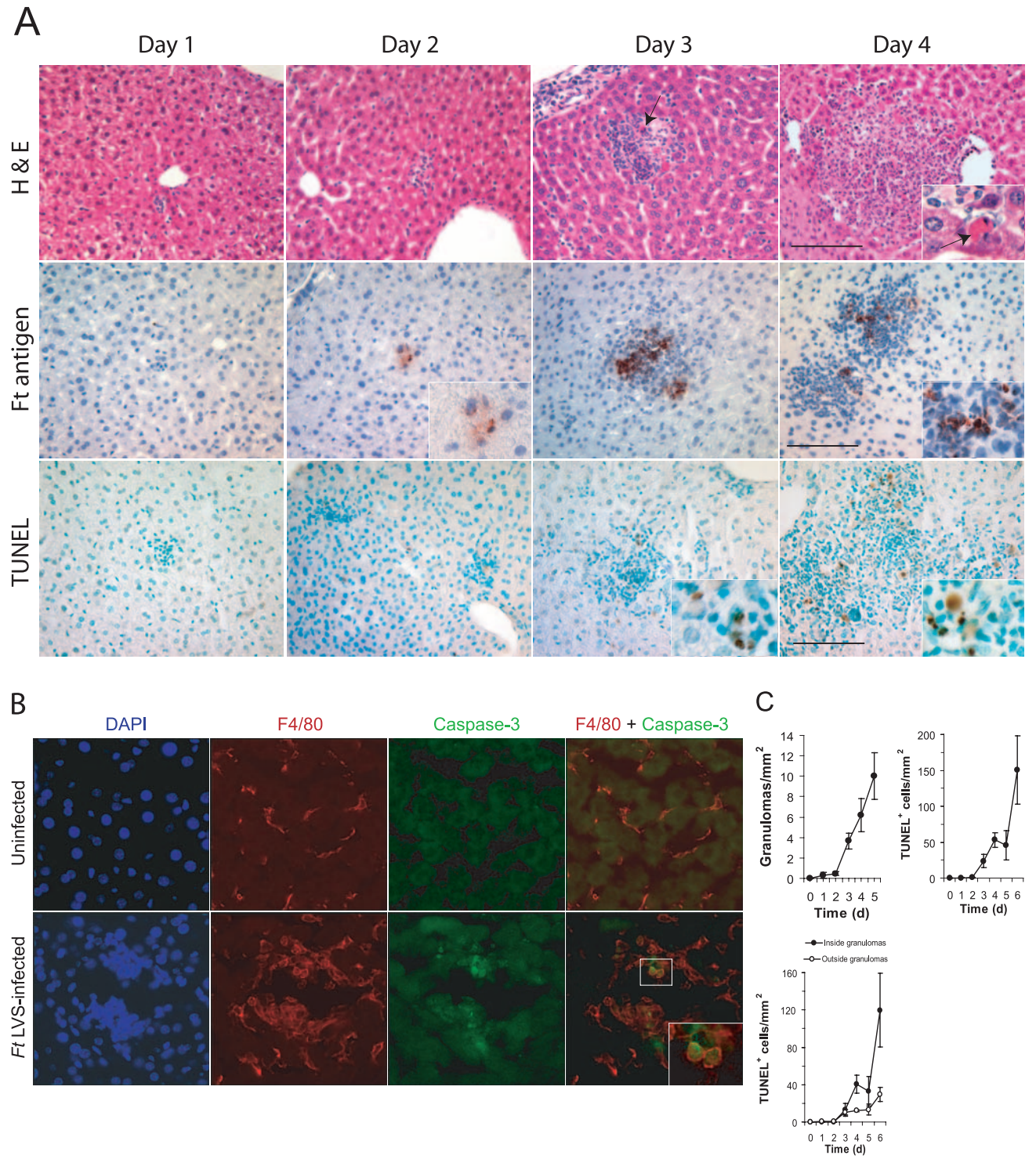

FIG. 2. Hepatic granuloma formation in *F. tularensis* LVS-infected mice. (A) Five mice per group were challenged i.n. with *F. tularensis* LVS and samples of their livers were collected at the indicated times. Fixed tissue samples were stained with hematoxylin and eosin (H&E) to show histopathology, anti-*Francisella* antigens (Ft antigen) to localize bacterial antigens, or TUNEL reagent to detect cells with double-strand DNA breaks. Note the dying cell with condensed, fragmented chromatin (arrow), the localization of *F. tularensis* LVS antigens both within the granuloma and occasionally within hepatocytes, and the TUNEL-positive cells concentrated within the granulomas. Bar, 100 μm. (B) Immunofluorescence imaging of a typical hepatic granuloma showing colocalization of activated caspase-3 with the macrophage marker F4/80. The frequency of caspase-3^+ cells within granulomas was 27.5 ± 11.2 cells/mm^2, while 9.2 ± 5.3 caspase-3^+ cells were detected outside the granulomas. (C) The frequencies of granulomas and TUNEL-positive cells increased significantly as a function of time postinfection ($P < 0.05$) (five mice per group). Granuloma frequency was not scored on day 6 postinfection due to the tendency of granulomas to merge with one another at this time. d, day.

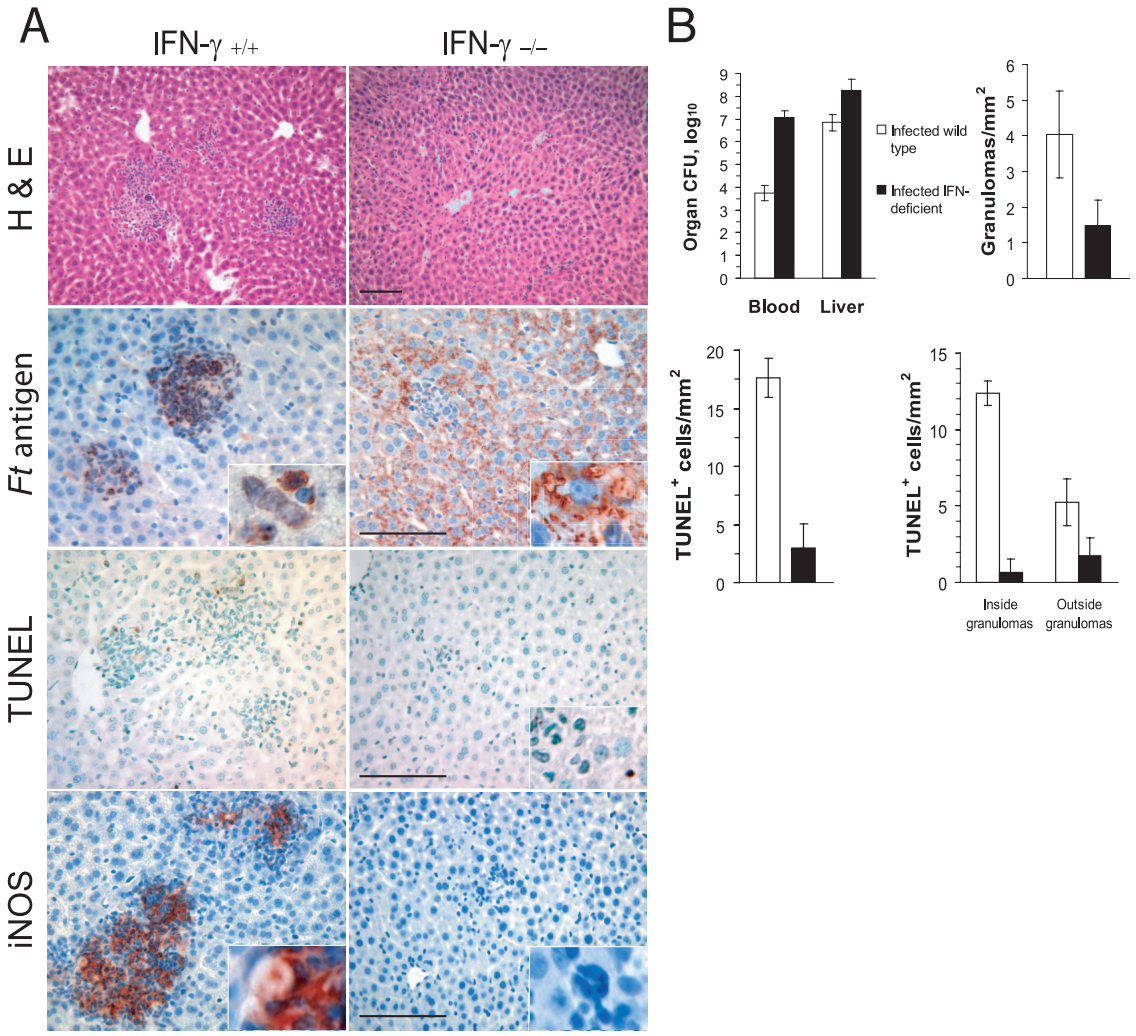

FIG. 3. IFN-γ is required for the formation and function of hepatic granulomas. (A) Wild-type C57BL/6J or coisogenic IFN-γ-deficient mice (four per group) were challenged i.n. with *F. tularensis* LVS, and their livers were recovered 4 days later. Shown is the effect of IFN-γ deficiency on the localization of *Francisella* antigens (*Ft* antigen) and TUNEL-positive cells and the expression of iNOS. H&E, hematoxylin and eosin staining. Bar, 100 μm. (B) Comparison of the bacterial burdens, frequencies of granulomas, and distribution of dying cells within the livers of infected wild-type and IFN-γ-deficient mice. The differences between the wild-type and IFN-γ-deficient mice were significant ($P < 0.05$) for all measurements, except for the densities of TUNEL$^+$ cells outside the granulomas.

tant mice. The frequency of TUNEL$^+$ cells was significantly reduced in IFN-γ-deficient mice, especially inside the granulomas (Fig. 3B). Thus, in the absence of IFN-γ, the failure to form granulomas was associated with an increased bacterial burden in the liver, a dispersed distribution of bacterial antigens, and a marked decrease in the numbers of cells containing double-strand DNA breaks.

The expression of iNOS in the *F. tularensis* LVS-infected mouse liver is IFN-γ dependent and contributes to the induction of cell death within granulomas. Cole et al. (3) showed that iNOS expression in the livers of mice infected with *F. tularensis* LVS by the intradermal route was limited to inflammatory granulomas. The current study confirms this finding and shows that the induction of iNOS in *F. tularensis* LVS infections is IFN-γ dependent (Fig. 3A). This spatial distribution of iNOS suggested that the enzyme might play a role in hepatic granuloma formation, the containment of infection within the granulomas, or the spatial distribution of cell death. To test these hypotheses, we compared the responses to infection of wild-type and iNOS-deficient mice (Fig. 4A). While the absence of iNOS expression resulted in a decreased frequency of granulomas (Fig. 4B), it did not lead to the dissemination of *F. tularensis* LVS antigens or an increase of liver bacterial burden, as was seen for infected IFN-γ-deficient mice. Mice deficient in iNOS did show significantly decreased densities of TUNEL$^+$ cells (Fig. 4B) both within and outside the granulomas. Thus, it appears that iNOS is an important mediator of cell death in the livers of *F. tularensis* LVS-infected mice, although iNOS does not mediate the spatial restriction of the pathogen within the granulomas.

Hepatic NK cells constitute a major source of IFN-γ during *F. tularensis* LVS infections. Having established the importance of IFN-γ in mediating the formation and functions of hepatic granulomas, we next asked whether the cytokine was

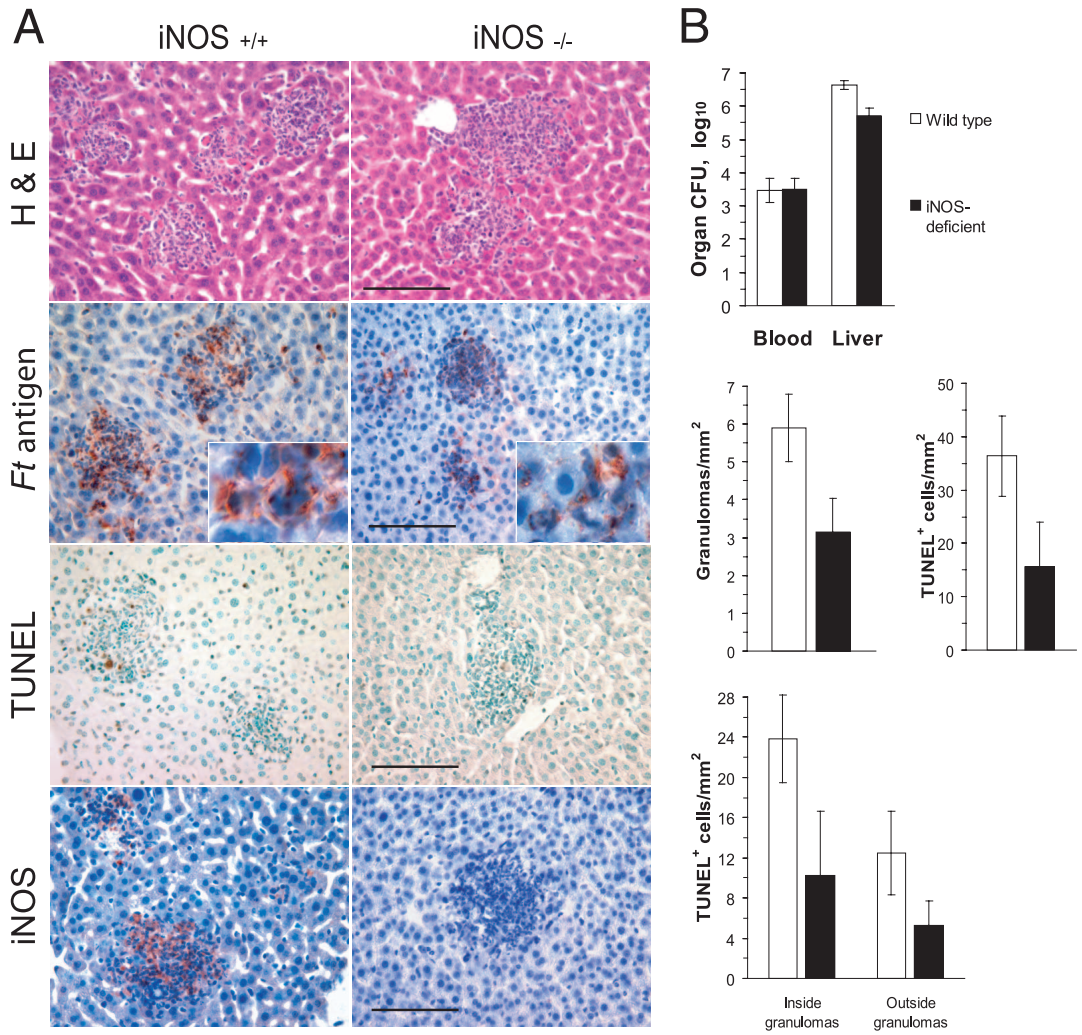

FIG. 4. The expression of iNOS is not required for restricting *F. tularensis* LVS to hepatic granulomas but does determine the frequency of dying cells in infected livers. (A) Liver samples that were obtained from mice (four mice per group) challenged i.n. with *F. tularensis* LVS were analyzed for the distribution of *Francisella* antigens (*Ft* antigen), TUNEL-positive cells, and iNOS-expressing cells. H&E, hematoxylin and eosin staining. Bars, 100 μm. (B) Tissue bacterial burdens, granuloma frequencies, and frequencies of TUNEL-positive cells in *F. tularensis* LVS-infected wild-type and iNOS-deficient mice. Compared to wild-type mice, iNOS-deficient mice had significantly low liver bacterial burdens, frequencies of granulomas, and frequencies of $TUNEL^+$ cells both inside and outside the granulomas ($P < 0.05$).

produced within the liver during *F. tularensis* LVS infection and by what cell type. Depending on the challenge dose, IFN-γ was detectable in the serum as early as the second day postinfection, reached a peak by day 4, and remained high for several days (Fig. 5A). To determine the cellular origin of the cytokine in infected animals, mononuclear cells were prepared from the lungs, spleen, lymph nodes, blood, and liver 4 days postinfection, and cells containing intracellular IFN-γ were enumerated by flow cytometry. While the highest frequency of cells expressing intracellular IFN-γ was present in the liver, large numbers of cytokine-producing cells were also detected in the lungs (Fig. 5B). The spleen contained a lower frequency of positive cells, and no IFN-γ-expressing cells were detected in the blood or lymph nodes (data not shown). In previous studies, perfusion of the liver by cannulating the portal vein did not decrease the frequency of IFN-γ^+ cells in the livers of infected mice (32), indicating that these cytokine-expressing cells were not simply blood-borne lymphocytes. Despite differences in the proportions of the various lymphocyte subsets within the different organs (Fig. 5B, middle row), NK cells ($NK1.1^+CD3\varepsilon^-$) constituted the largest fraction of IFN-γ-producing cells in all of the organs following i.n. challenge (Fig. 5B, bottom row). The remaining cells mediating pulmonary or hepatic IFN-γ production were predominantly T cells and NKT cells. Whereas challenge doses as low as 2 LD_{50} were sufficient to induce high-level IFN-γ production (Fig. 5C), the optimum response was seen when mice were challenged with 10^4 CFU. Under these conditions, 40% of the NK cells were activated for IFN-γ expression on day 4 postinfection.

Natural killer cells control the spatial distribution of *F. tularensis* LVS, iNOS, and cell death in the liver. Given the dominant role NK cells play in the hepatic IFN-γ response to *F. tularensis* LVS, we next asked whether the depletion of NK cells would alter responses to infection in a manner similar to

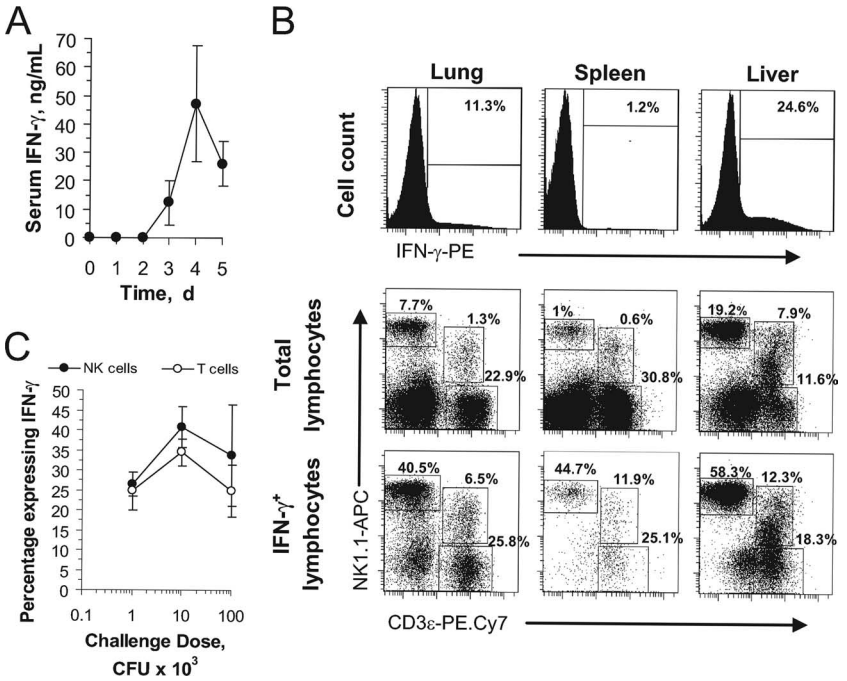

FIG. 5. The IFN-γ response to i.n. *F. tularensis* LVS challenge is mediated by pulmonary and hepatic NK cells. (A) Mice (five per group) were challenged i.n. with 3.6×10^3 CFU *F. tularensis* LVS bacteria, and circulating IFN-γ levels were measured from serum samples collected on the indicated days postinfection. d, day. (B) Mice were challenged i.n. with *F. tularensis* LVS, and mononuclear cells were prepared 4 days postchallenge. The cells expressing intracellular IFN-γ were enumerated by flow cytometry (top row). The surface phenotypes of the total mononuclear cells from each organ (middle row) or the IFN-γ-expressing subset of cells (bottom row) were determined by polychromatic flow cytometry. PE, phycoerythrin; APC, allophycocyanin. (C) The percentages of hepatic NK cells or T cells from i.n. challenged mice that expressed intracellular IFN-γ were determined by flow cytometry.

that seen for IFN-γ-deficient mice. To evaluate this, we compared wild-type mice to mice that were treated with anti-asialo-GM1. An additional control group of TCRβδ-deficient mice was also included. Treatment of mice with anti-asialo-GM1 resulted in a nearly complete depletion of both NK cells and NKT cells (Fig. 6A). The frequency of hepatic IFN-γ^+ cells and the concentration of serum IFN-γ in the NK cell-depleted group decreased by approximately 50% (Fig. 6C), and there were essentially no IFN-γ-producing NK or NKT cells detectable in their livers (Fig. 6A). By comparison, TCRβδ-deficient mice lacked both NKT cells and T cells and showed no IFN-γ production by these lymphocyte subsets when infected with *F. tularensis* LVS. However, their livers contained large numbers of IFN-γ-expressing NK cells.

Numerous $CD3^+$ cells were found within the granulomas of wild-type infected mice and localized near the outer boundaries of the granulomas, especially as these structures increased in size (Fig. 6B). A similar distribution of $CD3^+$ cells was seen for anti-asialo-GM1-treated mice, whereas TCRβδ-deficient mice lacked $CD3^+$ cells in their livers.

Selectively depleting either asialo-$GM1^+$ or TCR^+ hepatic lymphocytes did not greatly influence bacterial burdens in the liver on day 4 postinfection or the formation of hepatic microgranulomas (Fig. 6C). However, compared to wild-type or TCRβδ-deficient mice, NK cell-depleted mice showed high expression of *Francisella* antigens outside the granulomas, and extensive staining of hepatocytes was seen (Fig. 6B, inset). There was a large increase in the number of $TUNEL^+$ cells in the livers at this time in NK cell-depleted mice due primarily to an increase of cell death outside the granulomas. Specifically, most of the $TUNEL^+$ cells outside granulomas were concentrated within large areas of focal necrosis, particularly along the interface between necrotic and normal-appearing liver tissue (Fig. 6D). Very little inflammatory cell infiltration was observed for these areas, but there was extensive karyolysis typical of coagulation necrosis. This focal necrosis was not seen on day 4 postinfection for infected wild-type, TCRβδ-deficient, or IFN-γ-deficient mice.

With one exception, the depletion of NK cells from TCRβδ-deficient mice did not change these granuloma features beyond what was seen for wild-type mice that were treated with anti-asialo-GM1. Mice lacking NK, NKT, and T cells showed smaller and less frequent hepatic granulomas than wild-type mice (Fig. 6C) but otherwise resembled mice lacking NK and NKT cells. Both groups of immunodeficient mice showed a large increase in the frequency of dying cells outside the granulomas in areas of focal necrosis (Fig. 6C).

The pattern of iNOS expression in the livers of NK cell-depleted mice was also of interest (Fig. 6B). Instead of being spatially limited to the granulomas, iNOS was expressed by cells both within and outside the granulomas. The latter appeared to include Kupffer cells and sinusoidal endothelial cells. Thus, with the depletion of NK cells, bacterial antigens within the liver were seen outside the granulomas and both iNOS expression and cell death increased in the liver.

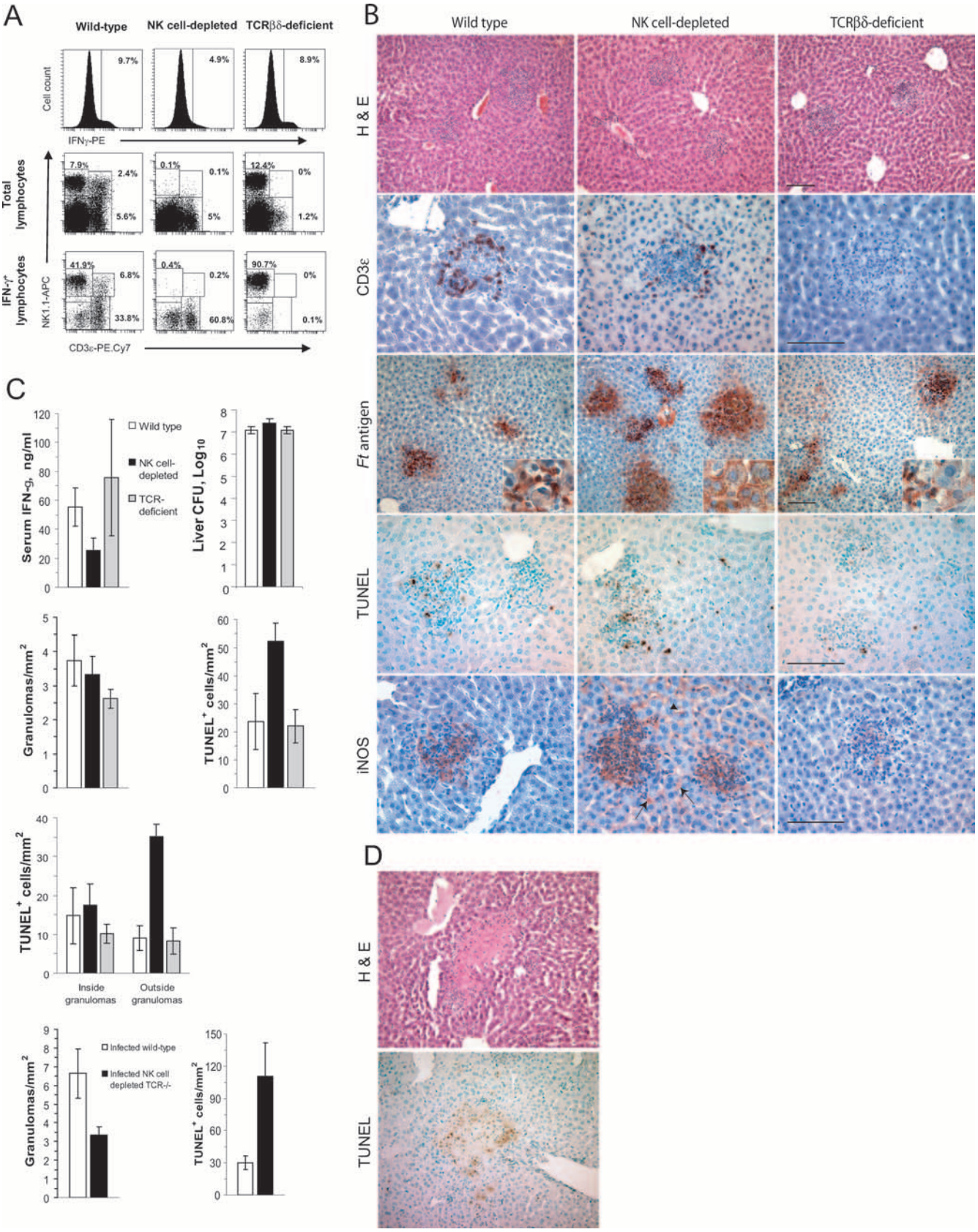

FIG. 6. Depletion of NK cells alters the functions of hepatic granulomas in *F. tularensis* LVS-infected mice. Wild-type, NK cell-depleted, or T-cell-deficient mice (five per group) were each challenged i.n. with *F. tularensis* LVS, and samples of their livers were recovered 4 days later.

DISCUSSION

IFN-γ produced in mice within the first few days of exposure to *F. tularensis* LVS is a key determinant in the course and outcome of the infection (1, 8, 9, 10, 19). Mutant IFN-γ-deficient mice (5, 8, 10) or immunocompetent mice treated with neutralizing antibodies to the cytokine (1, 9, 19) succumb at much lower challenge doses than do wild-type mice and show altered pathophysiological responses to the pathogen. In the present study, NK cells, NKT cells, and T cells were the principal sources of IFN-γ in the livers of mice with primary *F. tularensis* LVS infections. NK cells clearly constituted the largest fraction of IFN-γ-expressing cells in the liver, and depletion of these cells significantly decreased, but did not eliminate, hepatic IFN-γ expression. NK cells also comprised the most frequent IFN-γ-producing cell subset in the lungs after i.n. challenge, which is consistent with an earlier report by Lopez et al. (20).

Available evidence suggests that IFN-γ has a role in *F. tularensis* LVS infections that is more complex than simply serving as an activator of mononuclear phagocytes for intracellular killing of the pathogen. In the present study, we show that IFN-γ has multiple effects on the course of hepatic infections in mice. First, as reported by Chen et al. (2), who characterized mice infected with a virulent type B *F. tularensis* subsp. *holarctica* strain, IFN-γ was essential for the optimum formation of hepatic microgranulomas in *F. tularensis* LVS infections. In the absence of IFN-γ, many fewer granulomas were seen and these were much smaller than the granulomas observed for infected wild-type mice. How IFN-γ affects granuloma formation in *F. tularensis* LVS infections has not heretofore been described, but studies on this response in other infection models suggest that IFN-γ regulates chemokine expression and the recruitment of inflammatory cells (17, 21, 28). Whatever the mechanism, the pathogen itself is apparently not a sufficient stimulus for the formation of granulomas, because IFN-γ-deficient mice showed impaired granuloma formation in the liver despite increased levels of infection within the organ.

In the liver, IFN-γ-dependent granuloma formation is also essential for the spatial containment of *F. tularensis* LVS. In the absence of IFN-γ and normal granuloma function, *Francisella* antigens were widely distributed throughout the liver parenchyma, including extensive expression within hepatocytes. Conlan et al. (4, 6) first reported infection of mouse hepatocytes by a number of different *F. tularensis* strains, and Qin and Mann (24) recently showed that the type A *F. tularensis* Schu S4 strain infects and replicates within human HepG2 hepatoma cells. In the present study, widespread hepatic distribution of *Francisella* antigens was seen for IFN-γ-deficient mice and was accompanied by increased numbers of viable bacteria in the liver. This indicates that significantly more replication of the microbe occurred in the liver in the absence of the granuloma response.

The induction of granulomas and the spatial restriction of microbial infection within the liver appear to be two distinct responses to *F. tularensis* LVS. For example, depleting NK cells from mice had no effect on granuloma formation but did increase the appearance of *Francisella* antigens outside the granulomas. Thus, the partial reduction in hepatic IFN-γ production in NK cell-depleted mice was associated with the formation of "leaky" granulomas that failed to fully contain the infection. The same phenotype was observed for NK cell-depleted TCRβδ-deficient mice. While differences in the cellular constituents of granulomas in wild-type compared to NK cell-depleted mice may explain this effect, another interpretation is that the amount of IFN-γ required for granuloma formation is less than that necessary for preventing microbial dissemination.

A third IFN-γ-dependent response associated with hepatic granulomas was the induction of cell death within the liver. Numerous $TUNEL^+$ cells were found within granulomas of wild-type mice, particularly near the outer margins of these inflammatory foci. By contrast, the frequency of dying cells in the liver was markedly decreased for infected IFN-γ-deficient animals, despite a significant increase in bacterial burden in the organ. Because iNOS expression was both restricted to the granulomas and IFN-γ dependent, it was not surprising that *F. tularensis* LVS-infected, iNOS-deficient mice showed decreased numbers of $TUNEL^+$ cells in their livers. These findings suggest that cell death induced within hepatic granulomas represents a convergence of three responses to infection. The first is the recruitment of large numbers of phagocytic cells to the granulomas. The second may be intracellular infection per se, which is promoted by the retention of the bacteria within the granulomas. The third essential response appears to be the induction of iNOS, which may create a sufficiently prooxidant environment to signal the death of infected cells. In the liver, each of these processes was spatially restricted to the granulomas and regulated by IFN-γ. The finding that an early apoptosis marker, activated caspase-3, colocalized with $F4/80^+$ cells within the granulomas is consistent with this interpretation and the conclusion that infected macrophages constitute at least a portion of the dying cells.

Although the depletion of NK cells decreased IFN-γ pro-

(A) Hepatic mononuclear cells were analyzed by flow cytometry for the expression of intracellular IFN-γ (top row) and the presence of the major subsets of cells (middle row) or the three major subsets of lymphocytes or IFN-γ-producing cells (bottom row). PE, phycoerythrin; APC, allophycocyanin. (B) Granuloma formation and the distribution of CD3ε-expressing cells, *Francisella* antigens (*Ft* antigen), TUNEL-positive cells, and iNOS in the livers of infected mice. Note the presence of *Francisella* antigens within hepatocytes of NK cell-depleted mice and the expression of iNOS by Kupffer cells (arrow) and sinusoidal endothelial cells (arrowhead) of these animals. H&E, hematoxylin and eosin staining. (C) Serum IFN-γ concentrations, bacterial counts in the livers, and distribution of $TUNEL^+$ cells in infected mice. Mice depleted of NK cells had significantly more bacteria in their livers, higher totals of $TUNEL^+$ cells, and more $TUNEL^+$ cells outside the granulomas than did wild-type mice ($P < 0.05$). Mice lacking NK, NKT, and T cells showed a significant decrease in the frequency of granulomas ($P < 0.05$) and a significant increase in the frequency of $TUNEL^+$ cells in their livers ($P < 0.05$). (D) Dying cells within the livers of NK cell-depleted mice were found within areas of focal necrosis.

duction, granulomas still formed in the liver and the frequency of dying cells actually increased. On first consideration, this seems inconsistent with the findings obtained with infected IFN-γ-deficient mice. However, NK cell depletion did not eliminate IFN-γ expression by hepatic T cells, which were found within the granulomas. Indeed, even the hepatic mononuclear cells from TCR-deficient NK cell-depleted mice contained small numbers of $NK1.1^-$ $CD3^-$ IFN-γ^+ cells. However, the loss of NK cells changed the distribution of bacterial antigens, with a substantial increase in the expression of *Francisella* antigens outside the granulomas, including extensive expression within hepatocytes. The focal necrosis that accompanied this change was characterized by large numbers of cells showing pyknosis, karyorrhexis, or karyolysis and extensive TUNEL. This pattern of focal coagulation necrosis was not seen for either wild-type or T-cell-deficient mice at this stage of infection but is typical of the liver pathology observed for wild-type mice several days later. While this finding in no way diminishes the likely role of T cells in resolving *F. tularensis* LVS infections in mice, it indicates that the T cells are not essential for early granuloma formation or function in these infections.

Thus, the primary function of hepatic NK cells in *F. tularensis* LVS-infected mice appears to be in limiting the spread of infection beyond the granuloma. Once infection outside granulomas reached high levels in NK cell-depleted mice, extensive cell death followed. That a similar pattern did not occur in the IFN-γ-deficient mouse suggests that IFN-γ plays an essential role in this process. iNOS, whose expression in the liver was IFN-γ dependent, may mediate large-scale cell death induction in areas of focal necrosis, especially as the infection progresses. In NK cell-depleted mice, the pattern of iNOS expression was remarkably different from that seen for wild-type mice. In addition to its expression within the granulomas, iNOS was found throughout the liver parenchyma in Kupffer cells and sinusoidal endothelial cells. This pattern is typical of that seen for the mouse liver following challenge with purified endotoxic lipopolysaccharides (29). Thus, NK cells appear to play a key role in restricting *F. tularensis* LVS infection, iNOS expression, and cell death to the granulomas.

In contrast to Rasmussen et al. (25), we observed numerous $CD3^+$ cells within hepatic granulomas of *F. tularensis* LVS-infected mice as early as day 2 postinfection. As the granulomas grew, $CD3^+$ cells assumed positions near the outer boundaries of these structures, which are similar to the mantles of lymphocytes that form in tuberculous granulomas in mice and guinea pigs (22). Despite their proximity to $TUNEL^+$ cells in the granulomas, T cells did not appear to mediate cell death in the liver at these early time points. Both *F. tularensis* LVS-infected TCRβδ-deficient mice and infected perforin-deficient mice (data not shown) had normal numbers and distributions of $TUNEL^+$ cells in their livers on day 4 postinfection. These findings are consistent with the conclusion that early death induction within *F. tularensis* LVS-containing granulomas is much more dependent on IFN-γ expression and NK cells than perforin- and granzyme-dependent cytolytic mechanisms. Currently, we favor the interpretation that IFN-γ acts within granulomas by inducing iNOS expression, which together with intracellular *F. tularensis* LVS infection signals cell death. The role of NK cells is more complex but seems to include facilitating the containment of the infection and spatially limiting the expression of iNOS within the granulomas.

There are significant differences between the pathological responses of mice infected with the attenuated LVS strain of *F. tularensis* subsp. *holarctica* and animals infected with highly virulent strains of *F. tularensis* subsp. *tularensis* (type A). While minimum lethal doses (e.g., 10 CFU given by the i.n. route) of certain type A strains induced the early formation of similar-appearing hepatic microgranulomas in C57BL/6 mice, these structures rapidly become necrotic and unrecognizable by day 4 postinfection (S. M. Bokhari and M. J. Parmely, unpublished data). Unfortunately, similar information on early granuloma responses during infections with type A *F. tularensis* strains in human beings is not available, and most of what we know about the pathological changes during human tularemia is derived from studying autopsy specimens. Because experimental mouse tularemia caused by type A *F. tularensis* strains progresses so rapidly, many of the cells and immune mediators that regulate early hepatic responses to *F. tularensis* LVS may not play a similar role with these virulent organisms. Identifying which of the processes that regulate granuloma formation and function in *F. tularensis* LVS infections are not seen during type A *F. tularensis* infections will provide important insight about the ability of virulent organisms to evade immune elimination.

ACKNOWLEDGMENTS

We thank Gregory Vanden Heuvel for his assistance with photomicroscopy, Rosetta Barkley and Jing Huang for their technical assistance, and Jason Wickstrum for his comments. We are also grateful to Bill Narayan for his support and careful review of the manuscript.

This work was supported by NIH grants R21 AI062939 and P20 RR016443 and a bridging grant from the University of Kansas Medical Center Research Institute. S.M.B. is a recipient of a Biomedical Research Scholars Program fellowship.

REFERENCES

1. **Anthony, L. S., E. Ghadirian, F. P. Nestel, and P. A. Kongshavn.** 1989. The requirement for gamma interferon in resistance of mice to experimental tularemia. Microb. Pathog. **7:**421–428.
2. **Chen, W., R. KuoLee, H. Shen, and J. W. Conlan.** 2004. Susceptibility of immunodeficient mice to aerosol and systemic infection with virulent strains of Francisella tularensis. Microb. Pathog. **36:**311–318.
3. **Cole, L. E., K. L. Elkins, S. M. Michalek, N. Qureshi, L. J. Eaton, P. Rallabhandi, N. Cuesta, and S. N. Vogel.** 2006. Immunologic consequences of Francisella tularensis live vaccine strain infection: role of the innate immune response in infection and immunity. J. Immunol. **176:**6888–6899.
4. **Conlan, J. W., W. Chen, H. Shen, A. Webb, and R. KuoLee.** 2003. Experimental tularemia in mice challenged by aerosol or intradermally with virulent strains of Francisella tularensis: bacteriologic and histopathologic studies. Microb. Pathog. **34:**239–248.
5. **Conlan, J. W., R. KuoLee, H. Shen, and A. Webb.** 2002. Different host defences are required to protect mice from primary systemic vs pulmonary infection with the facultative intracellular bacterial pathogen, Francisella tularensis LVS. Microb. Pathog. **32:**127–134.
6. **Conlan, J. W., and R. J. North.** 1992. Early pathogenesis of infection in the liver with the facultative intracellular bacteria *Listeria monocytogenes*, *Francisella tularensis*, and *Salmonella typhimurium* involves lysis of infected hepatocytes by leukocytes. Infect. Immun. **60:**5164–5171.
7. **De Rosa, S. C., J. M. Brenchley, and M. Roederer.** 2003. Beyond six colors: a new era in flow cytometry. Nat. Med. **9:**112–117.
8. **Duckett, N. S., S. Olmos, D. M. Durrant, and D. W. Metzger.** 2005. Intranasal interleukin-12 treatment for protection against respiratory infection with the *Francisella tularensis* live vaccine strain. Infect. Immun. **73:**2306–2311.
9. **Elkins, K. L., T. Rhinehart-Jones, C. A. Nacy, R. K. Winegar, and A. H. Fortier.** 1993. T-cell-independent resistance to infection and generation of immunity to *Francisella tularensis*. Infect. Immun. **61:**823–829.
10. **Elkins, K. L., T. R. Rhinehart-Jones, S. J. Culkin, D. Yee, and R. K. Winegar.** 1996. Minimal requirements for murine resistance to infection with *Francisella tularensis* LVS. Infect. Immun. **64:**3288–3293.

11. **El-Zammar, O. A., and A. L. Katzenstein.** 2007. Pathological diagnosis of granulomatous lung disease: a review. Histopathology **50:**289–310.
12. **Fortier, A. H., M. V. Slayter, R. Ziemba, M. S. Meltzer, and C. A. Nacy.** 1991. Live vaccine strain of *Francisella tularensis*: infection and immunity in mice. Infect. Immun. **59:**2922–2928.
13. **Fuller, C. L., J. L. Flynn, and T. A. Reinhart.** 2003. In situ study of abundant expression of proinflammatory chemokines and cytokines in pulmonary granulomas that develop in cynomolgus macaques experimentally infected with *Mycobacterium tuberculosis*. Infect. Immun. **71:**7023–7034.
14. **Heninger, E., L. H. Hogan, J. Karman, S. Macvilay, B. Hill, J. P. Woods, and M. Sandor.** 2006. Characterization of the Histoplasma capsulatum-induced granuloma. J. Immunol. **177:**3303–3313.
15. **Ishiguro, T., M. Naito, T. Yamamoto, G. Hasegawa, F. Gejyo, M. Mitsuyama, H. Suzuki, and T. Kodama.** 2001. Role of macrophage scavenger receptors in response to Listeria monocytogenes infection in mice. Am. J. Pathol. **158:**179–188.
16. **Jakubzick, C., H. Wen, A. Matsukawa, M. Keller, S. L. Kunkel, and C. M. Hogaboam.** 2004. Role of CCR4 ligands, CCL17 and CCL22, during Schistosoma mansoni egg-induced pulmonary granuloma formation in mice. Am. J. Pathol. **165:**1211–1221.
17. **Kamijo, R., J. Le, D. Shapiro, E. A. Havell, S. Huang, M. Aguet, M. Bosland, and J. Vilcek.** 1993. Mice that lack the interferon-gamma receptor have profoundly altered responses to infection with bacillus Calmette-Guerin and subsequent challenge with lipopolysaccharide. J. Exp. Med. **178:**1435–1440.
18. **Lamps, L. W., J. M. Havens, A. Sjostedt, D. L. Page, and M. A. Scott.** 2004. Histologic and molecular diagnosis of tularemia: a potential bioterrorism agent endemic to North America. Mod. Pathol. **17:**489–495.
19. **Leiby, D. A., A. H. Fortier, R. M. Crawford, R. D. Schreiber, and C. A. Nacy.** 1992. In vivo modulation of the murine immune response to *Francisella tularensis* LVS by administration of anticytokine antibodies. Infect. Immun. **60:**84–89.
20. **Lopez, M. C., N. S. Duckett, S. D. Baron, and D. W. Metzger.** 2004. Early activation of NK cells after lung infection with the intracellular bacterium, Francisella tularensis LVS. Cell. Immunol. **232:**75–85.
21. **Murray, H. W.** 2001. Tissue granuloma structure-function in experimental visceral leishmaniasis. Int. J. Exp. Pathol. **82:**249–267.
22. **Oliver, C. T., R. J. Basaraba, A. A. Frank, and I. M. Orne.** 2003. Granuloma formation in mouse and guinea pig models of experimental tuberculosis, p. 65–84. *In* D. L. Boros (ed.), Granulomatous infections and inflammations: cellular and molecular mechanisms. ASM Press, Washington, DC.
23. **Perfetto, S. P., P. K. Chattopadhyay, and M. Roederer.** 2004. Seventeen-colour flow cytometry: unravelling the immune system. Nat. Rev. Immunol. **4:**648–655.
24. **Qin, A., and B. J. Mann.** 2006. Identification of transposon insertion mutants of Francisella tularensis tularensis strain Schu S4 deficient in intracellular replication in the hepatic cell line HepG2. BMC Microbiol. **6:**69.
25. **Rasmussen, J. W., J. Cello, H. Gil, C. A. Forestal, M. B. Furie, D. G. Thanassi, and J. L. Benach.** 2006. Mac-1+ cells are the predominant subset in the early hepatic lesions of mice infected with *Francisella tularensis*. Infect. Immun. **74:**6590–6598.
26. **Roach, D. R., A. G. Bean, C. Demangel, M. P. France, H. Briscoe, and W. J. Britton.** 2002. TNF regulates chemokine induction essential for cell recruitment, granuloma formation, and clearance of mycobacterial infection. J. Immunol. **168:**4620–4627.
27. **Sato, N., W. A. Kuziel, P. C. Melby, R. L. Reddick, V. Kostecki, W. Zhao, N. Maeda, S. K. Ahuja, and S. S. Ahuja.** 1999. Defects in the generation of IFN-gamma are overcome to control infection with Leishmania donovani in CC chemokine receptor (CCR) 5-, macrophage inflammatory protein-1 alpha-, or CCR2-deficient mice. J. Immunol. **163:**5519–5525.
28. **Squires, K. E., R. D. Schreiber, M. J. McElrath, B. Y. Rubin, S. L. Anderson, and H. W. Murray.** 1989. Experimental visceral leishmaniasis: role of endogenous IFN-gamma in host defense and tissue granulomatous response. J. Immunol. **143:**4244–4249.
29. **Wang, F., L. Y. Wang, D. Wright, and M. J. Parmely.** 1999. Redox imbalance differentially inhibits lipopolysaccharide-induced macrophage activation in the mouse liver. Infect. Immun. **67:**5409–5416.
30. **Warmington, K. S., L. Boring, J. H. Ruth, J. Sonstein, C. M. Hogaboam, J. L. Curtis, S. L. Kunkel, I. R. Charo, and S. W. Chensue.** 1999. Effect of C-C chemokine receptor 2 (CCR2) knockout on type-2 (schistosomal antigen-elicited) pulmonary granuloma formation: analysis of cellular recruitment and cytokine responses. Am. J. Pathol. **154:**1407–1416.
31. **Wickstrum, J. R., K. J. Hong, S. Bokhari, N. Reed, N. McWilliams, R. T. Horvat, and M. J. Parmely.** 2007. Coactivating signals for the hepatic lymphocyte gamma interferon response to *Francisella tularensis*. Infect. Immun. **75:**1335–1342.
32. **Zhang, G., R. D. Nichols, M. Taniguchi, T. Nakayama, and M. J. Parmely.** 2003. Gamma interferon production by hepatic NK T cells during *Escherichia coli* infection is resistant to the inhibitory effects of oxidative stress. Infect. Immun. **71:**2468–2477.

Editor: J. L. Flynn